Mathematical Biosciences and Engineering

MBE, 18(4): 4212–4225.
DOI: 10.3934/mbe.2021211
Received: 20 March 2021
Accepted: 12 May 2021
Published: 17 May 2021

http://www.aimspress.com/journal/MBE

Research article

Biomechanical responses of the cornea after small incision lenticule extraction (SMILE) refractive surgery based on a finite element model of the human eye

Yinyu Song, Lihua Fang*, Qinyue Zhu, Ruirui Du, Binhui Guo, Jiahui Gong and Jixia Huang

Key Laboratory of Nondestructive Test (Ministry of Education), Nanchang Hangkong University, Nanchang 330063, China

*** Correspondence:** Email: fanglh71@126.com; Tel: +8618170938193.

Abstract: *Purpose:* To investigate the biomechanical responses of the human cornea after small incision lenticule extraction (SMILE) procedures, especially their effects of SMILE surgery on stress and strain. *Methods:* Based on finite element analysis, a three-dimensional (3D) model of the human eye was established to simulate SMILE refractive surgery procedures. Stress and strain values were calculated by inputting the intraocular pressure (IOP). *Results:* After SMILE refractive surgery procedures, the stress and strain of the anterior and posterior corneal surfaces were significantly increased. The equivalent stress and strain on the anterior and posterior corneal surfaces increased with increasing diopter and were concentrated in the central area, whereas the values of stress and strain at the incision site on the anterior surface of the cornea were approximately 0. Compared with the anterior corneal surface, the stress and strain of the posterior surface were larger. Increasing IOP caused an approximately linear change in stress and a nonlinear increase in corneal strain. In addition, we found that the incision sizes and direction had less of an influence on stress and strain. In summary, SMILE surgery increased the equivalent stress and strain on the human cornea. *Conclusions:* The equivalent stress and strain of the anterior and posterior human corneal surfaces increased after SMILE refractive surgery; these increases were particularly noticeable on the posterior surface of the cornea.

Keywords: biomechanical responses; finite element model; SMILE; stress; strain

1. Introduction

The incidence of myopia is increasing yearly and has become a global public health problem [1]. Corneal refractive surgery is an one of the important way of treating refractive errors. To change the refractive ability of the eye, many refractive surgery techniques have been developed [2]. SMILE refractive surgery has emerged as a new surgical approach. It differs from Laser-assisted in situ keratectomy (LASIK) surgery because no corneal flap is created, and the corneal lenticule is extracted through a small incision. Because it is flapless and creates only a small incision, SMILE surgery is safer. The most important advantage of SMILE over LASIK is that it leaves the cornea with greater tensile strength [3], causing less damage to corneal biomechanics [4]. Therefore, SMILE has become the new choice for myopia correction procedures in traditional refractive surgery.

Corneal refractive surgery cuts corneal tissue to correct vision, and it has influence on the biomechanics of the corneal. Gyldenkerne et al. [4] confirmed that the curvature of the anterior corneal surface changed significantly after SMILE refractive surgery. Wei et al. [5] found that refractive surgery changed corneal structure and biomechanics. The stress and strain on cornea also increased after refractive surgery. Scarcelli et al. [6] showed that tensile tests were strongly correlated with the biomechanical properties of the cornea and the depth of the matrix. Knox et al. [7] found that the corneal stress changed after the incision was created in LASIK surgery. Franus [8] also studied the stress and strain of the cornea after LASIK. In addition, the main physiological function of the cornea is refraction, accounting for 70% of the refractive power of the eye [9]. And visual quality is closely related to corneal biomechanics after refractive surgery. Therefore, it is necessary to explore the postoperative characteristics of corneal stress and strain.

The finite element analysis method is a useful tool for calculating geometric, biomechanical and structural characteristics of biological [10]. Since the mid-20th century, its practicability has been verified in many fields. The method has been widely used in structural and fluid research and has been used to solve complex research problems [11]. Ariza-Gracia et al. [12] used the Gasser-Holzapfel-Ogden (GHO) constitutive model for finite element simulation of the human cornea. Kaliske et al. [13] described the viscoelastic material model. Anderson et al. [14] proposed the anisotropy model of the corneal shell. Pinsky et al. [15] applied the numerical model of anisotropy of corneal and scleral mechanics in surgery. In brief, the finite element analysis could accurately assess postoperative corneal biomechanics. Based on previous studies, we established a three-dimensional (3D) finite element whole-eye model to simulate SMILE refractive surgery to study postoperative changes in corneal stress and strain and provide valuable theoretical data for the diagnosis of ophthalmic diseases.

Corneal refractive surgery is predictable and stable [16]. However, the biomechanics become weaker and the vision problems, such as corneal thinning, myopia aggravation, and visual acuity decline still occur [17]. John et al. [18] found that the biomechanical properties of corneal reduced after SMILE and LASIK surgery, and the lower myopic had more tensile strength in SMILE procedure. Osman et al. [19] also confirmed that a retrospective study showed less reduction in corneal biomechanical properties of SMILE compared with the LASIK group. Peinado et al. [20] indicated that corneal distention caused by biomechanical impacted the whole corneal structure. Randleman et al. [17] showed that refractive surgery in which the cornea was cut might reduce the biomechanical stability of the cornea, even causing the complication of iatrogenic keratectasia. Cordero-Mendieta showed that corneal biomechanics had a great impact on the ophthalmological

studies. For this reason, we used finite element analysis to study the biomechanical characteristics of cornea after SMILE surgery.

Our study aims to evaluate postoperative corneal equivalent stress and strain. A 3D finite element model was constructed to simulate SMILE surgery. By loading IOP, the postoperative change in corneal strain and stress were explored through diopter, IOP, and incision sizes to explore the mechanism of how SMILE influences corneal biomechanics. It was not only important for preoperative diagnosis of eye disease, but also provided effective preventive measures for postoperative complications such as keratoconus.

2. Methods

2.1. The finite element method of the human eye

We used Siemens NX (Siemens AG, Munich, Germany) to build a 3D full-eye model of the human eye. According to the anterior surface of cornea and the thickness and size of the cornea cap, the point cloud data on the subsurface of the cornea cap were obtained. Then, the point cloud data were used to subtract the thickness of lenticule calculated by the Munnerlyn equation to simulate the removal of a corneal lenticule. After the corneal lenticule was removed, the lenticule interfaces were fitted the residual cornea by modifying the upper and lower surfaces of cornea cap and the postoperative SMILE eye model was constructed. The eye model consisted of a corneal cap, cornea and sclera. And the small incision was located at the junction of cornea cap and cornea, with a size of about 3 mm.

The IOP was loaded inner surface the eyeball, which was a fluid cavity with the eye as an enclosed inner surface. And the model was restrained in posterior scleral nerves that were surrounded by optic nerve bundle and biological tissues. In order to prevent rigid-body movement in the eye model, the force of fixation from the posterior scleral nerve was used as the the boundary conditions of model. In addition, the cornea and sclera, corneal cap and cornea were set as bond-connected, respectively. The lenticule interfaces and residual cornea were connected in frictionless way. Figure 1 was the diagram of the human eye model.

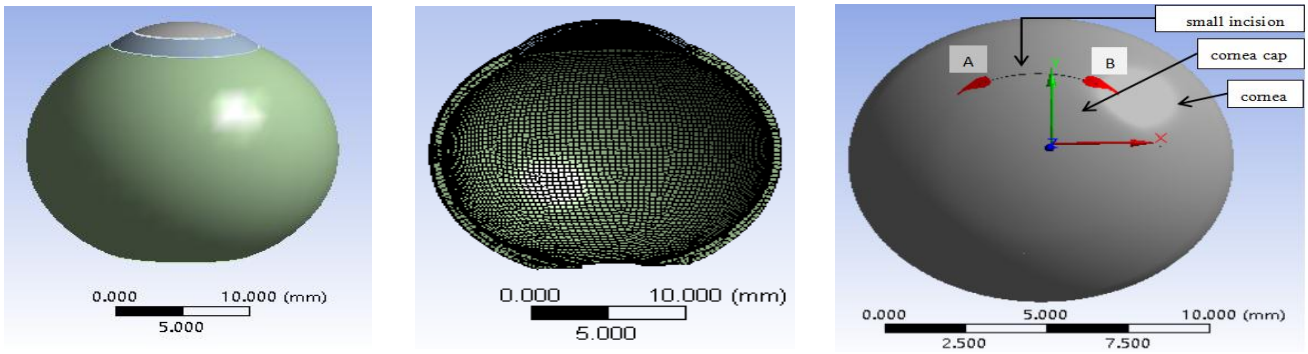

(a) (b) (c)

Figure 1. (a) The 3D whole-eye model. (b) The cross-sectional view of the model mesh. (c) The diagram of small incision model, the location of the small incision was the arc between the dots A and B, and the size was about 3 mm. The radii of curvature of the anterior and posterior corneal surfaces were 7.7 mm, 6.8 mm, respectively. The central corneal thickness was 0.5 mm, and the refractive index of the cornea was 1.376.

Meshing a model is a critical step in finite element analysis. The mesh quality of the model affects the calculation rate and the accuracy of the experimental data. In our study, the cornea cap, cornea and sclera were divided by tetrahedral and hexahedral meshes, respectively, and the mesh mass of the eye model was about 0.7. For the models of different diopters, the number of elements and nodes were slightly different, but the changes were not significant. The numbers of corneal nodes, corneal mesh cells, scleral nodes, and scleral mesh cells were 175,765, 59,104, 112,038, and 31,346, respectively.

2.2. Material properties

Grytz et al. [21] showed that the cornea and sclera were nonlinear material properties. In the establishment of the mathematical model of the eye, the Ogden strain-energy function [22] was used to represent the isotropy, hyperelasticity and incompressibility of the cornea and sclera. The specific formula can be expressed as follows:

$$W = \sum_{i=1}^{N} \frac{\mu_i}{\beta_i} (\bar{\lambda}_1^{\beta_i} + \bar{\lambda}_2^{\beta_i} + \bar{\lambda}_3^{\beta_i} - 3) + \sum_{k=1}^{N} \frac{1}{d_k} (J-1)^{2k} \tag{1}$$

Where β_i, μ_i and d_k are material constants, the determinant of the elastic deformation gradient is $J = \lambda_1 \lambda_2 \lambda_3$, the principal stretch are λ_1, λ_2, λ_3, respectively. And the deviatoric principal stretches is $\bar{\lambda}_i = J^{-1/3}\lambda_i$.

The shear modulus μ is defined by the following equation:

$$\mu = \frac{\sum_{i=1}^{N} \beta_i \mu_i}{2} \tag{2}$$

The bulk modulus K is defined by:

$$K = \frac{2}{d_1} \tag{3}$$

Due to the near incompressibility of the cornea and sclera, d_1 was about 0. According to the results of previous studies and material fitting of our study, N = 2 and N = 1 were independently selected as corneal and scleral fitting parameters, respectively, where corneal fitting parameters were as follows: μ_1 = 0.0034801 MPa, a_1 = 104.06, μ_2 = 0.0034801 MPa, and a_2 = 103.94. The scleral fitting parameters were as follows: μ_1 = 0.030224 MPa, and a_1 = 182.73.

3. **Simulation of SMILE refractive surgery**

SMILE creates a corneal lenticule that changes the surface curvature of the cornea to correct refractive errors. The thickness of the corneal lenticule was calculated based on the Munnerlyn equation in our study [23], the formula is defined by:

$$l_s(x,y)=\sqrt{\left(\sqrt{R_{ix}^2-x^2}+R_{iy}-R_{ix}\right)^2-y^2}$$
$$-\sqrt{R_f^2-x^2-y^2}+\sqrt{R_f^2-(O_z/2)^2} \quad (4)$$
$$+R_{ix}-R_{iy}-\sqrt{R_{ix}^2-(O_z/2)^2}$$

R_{ix} and R_{iy} are the preoperative radii of curvature of two major meridians of the anterior corneal surface, and their values are both 7.7 mm. R_f is the postoperative radius of curvature. O_Z represents the X-axis diameter of the optical zone. R_f can be expressed as:

$$R_f=\frac{1000(n-1)R_{ix}}{(n-1)+D_sR_{ix}} \quad (5)$$

where D_s and n are the myopic refraction in diopters and the refractive index of the cornea, respectively.

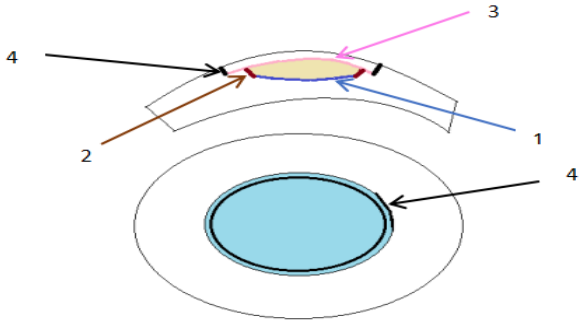

Figure 2. The simplified schematic diagram of the small incision lenticule extraction procedure. The lenticule cut was 1. The lenticule side cuts 2 was made. The cap interface was 3. The lenticule interfaces were created. Then the lenticule was removed through the small incision 4.

Figure 2 showed the principles of the SMILE procedure. Firstly, the corneal lenticule was made through incisions 1 and 2; then the corneal cap was made through incision 3; and finally, 3-mm small incision 4 was created, and the lenticule was extracted via the incision. In our study, the corrected refractions were related to the ablated corneal stromal lenticule, which was given by the ablation formula. The thickness of the corneal cap was 110 μm, and the diameters of the corneal cap and optical zone were 7.6 and 6.6 mm, respectively. After inputting the IOP, the equivalent stress and strain of the anterior and posterior surfaces of the cornea were calculated using the finite element software Ansys (Ansys, Canonsburg, PA, USA). We could investigate the effects of corrected diopters, IOP, and small-incision sizes on equivalent stress and strain.

4. Postoperative stress and strain of the cornea

As the cornea thins, the stress distribution becomes less uniform, and the cornea deforms by increasing corneal curvature in the thinner higher stress region to reduce local stress [24]. Based on finite element analysis, we used Ansys software to analyze the stress and strain of the cornea equivalent to that occurring after SMILE refractive surgery. Corneal deformation was observed after SMILE, and the equivalent stress could represent the stress inside the eyeball. To make the

calculation more accurate, the stress on the surface of the cornea in the X, Y, and Z directions were denoted as σ_x, σ_y, and σ_z, respectively. Then the stress can be expressed by the following formula:

$$(\sigma_x - \sigma_y)^2 + (\sigma_x - \sigma_z)^2 + (\sigma_y - \sigma_z)^2 = 2\sigma_s = 6k^2 \tag{6}$$

It can be rewritten as:

$$\sigma_s = \frac{\sqrt{2}}{2}\sqrt{(\sigma_x - \sigma_y)^2 + (\sigma_x - \sigma_z)^2 + (\sigma_y - \sigma_z)^2} \tag{7}$$

The equivalent stress is that the complex stress from the model of cornea equivalent to the stress in unidirectional stretching, the σ_e can be expressed as :

$$\sigma_e = \frac{\sqrt{2}}{2}\sqrt{(\sigma_x - \sigma_y)^2 + (\sigma_x - \sigma_z)^2 + (\sigma_y - \sigma_z)^2 + 6(\tau_{xy}^2 + \tau_{yz}^2 + \tau_{zx}^2)} \tag{8}$$

From the Mises yield conditions,$\sigma_e = \sigma_s$, we obtain:

$$\sigma_e = \sigma_s = \frac{\sqrt{2}}{2}\sqrt{(\sigma_x - \sigma_y)^2 + (\sigma_x - \sigma_z)^2 + (\sigma_y - \sigma_z)^2} \tag{9}$$

Then, its strain increment $d\varepsilon_e$ is computed as

$$d\varepsilon_e = \frac{\sqrt{(d\varepsilon_x - d\varepsilon_y)^2 + (d\varepsilon_y - d\varepsilon_z)^2 + (d\varepsilon_x - d\varepsilon_z)^2 + 6(d\gamma_{xy}^2 + d\gamma_{xz}^2 + d\gamma_{yz}^2)}}{\sqrt{2}(1+v')} \tag{10}$$

The equivalent strain can be obtained by the equation:

$$\varepsilon_e = \frac{1}{1+v'}\sqrt{\frac{1}{2}\left[(\varepsilon_x - \varepsilon_y)^2 + (\varepsilon_y - \varepsilon_z)^2 + (\varepsilon_x - \varepsilon_z)^2\right]} \tag{11}$$

where v` is Poisson's ratio of the eyeball material. Poisson ratio values for the human cornea ranges from 0.42 to 0.5, which indicates that the cornea tissue is nearly incompressible. A value of 0.49 was assumed in this study.

5. Results

5.1. Effect of corrected diopters on corneal surface equivalent stress

After setting material parameters and the mesh of the eyeball model, the IOP was loaded to simulate SMILE surgery. Considering the small incision was located in the Y-axis direction of the eye model, the equivalent stress in the Y-axis direction on the anterior and posterior corneal surfaces was calculated. In this part of the study, the influence of corrected diopters on corneal stress was explored. The optical zone diameter was 6.6 mm, and the diopter ranged from −1D to −15D, with an interval of 1 diopter. Figure 3 showed the relationship between corneal stress and myopic diopter.

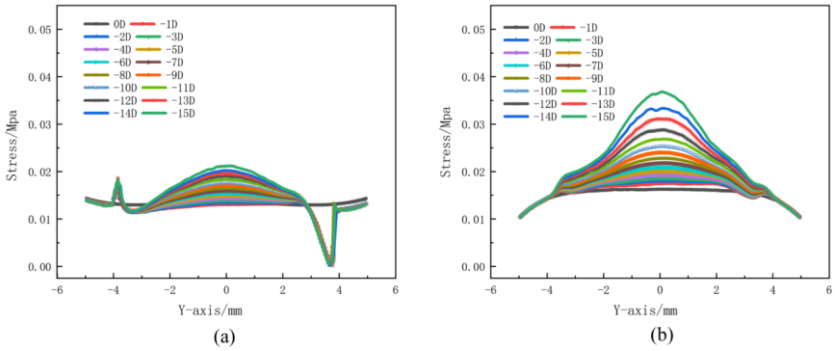

Figure 3. (a) Equivalent stress on the anterior surface of cornea under different corrected diopters. (b) Equivalent stress on the posterior surface of cornea under different corrected diopters. The corneal cap thickness was assumed to be 110 μm and the size was 7.6 mm, IOP was 15 mmHg. The diopter ranged from 0D to −15D.

Overall, compared with preoperative stress, the stress on the corneal anterior and posterior surfaces increased with increasing diopter, showing a regional distribution in the central region. As observed in Figure 3a, a small peak in stress occurred at −3.85 mm on the Y-axis. When the diopter was −15D, the stress reached its peak value of 0.019 MPa. The reason for this was that the corneal cap and cornea were in separated forms during construction, and stress concentration occured at their junctions. And at 3.8 mm on the Y-axis, the stress value dropped to 0.007 MPa. From Figure 3b, we concluded that the stress on the posterior surface of the cornea also increased with an increase in the corrected diopter and was concentrated in the central area. However, it showed a symmetrical distribution. When the corrected diopters were 0D and −15D, the stresses at the center of the cornea were 0.016 and 0.036 MPa, respectively. The stress value of −15D was about twice that of 0D. In addition, the stress on the posterior surface of the cornea showed no stress concentration phenomenon and changed more than that on the anterior surface.

5.2. Effect of corrected diopter on corneal surface equivalent strain

By loading IOP, we utilized the same method to obtain the equivalent strain on the anterior and posterior corneal surfaces. Figure 4 showed the relationship curves between strain and myopic diopter, where the diopter ranged from 0D to −15D.

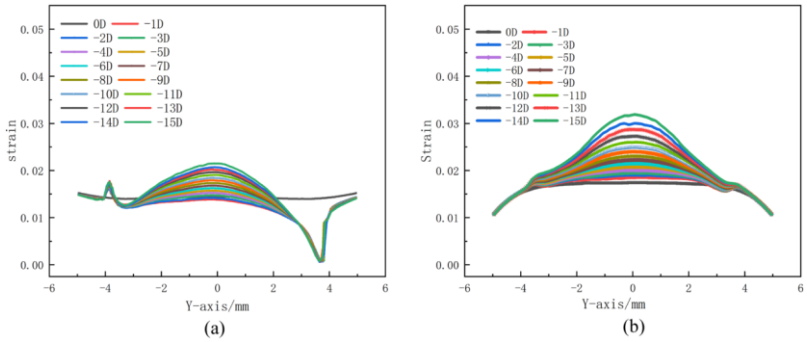

Figure 4. (a) Equivalent strain on the anterior surface of cornea under different corrected diopters. (b) Equivalent strain on the posterior surface of cornea under different corrected diopters. The corneal cap thickness was assumed to be 110 μm and the size was 7.6 mm, IOP was 15 mmHg. The diopter ranged from 0D to −15D.

According to Figure 4, the variation in corneal strain showed a similar pattern to that of stress. With increasing diopter, the strain increased and became more concentrated in the central area. As indicated by Figure 4a, the strain reached a small peak value at −3.85 mm with a maximum value of 0.18. At 3.8 mm, a sudden drop in strain to 0.009 occurred due to the small incision. Overall, the strain of the cornea increased with increased diopter and changed obviously at the site of incision. Figure 4b showed that the posterior surface strain of the cornea increased with a change of diopter. However, no sudden change in the strain occurred at the location of the incision. In addition, it changed more than that of the anterior surface.

5.3. Effect of IOP on corneal surface equivalent stress

The 3D finite element eye model with a diopter of −6D was loaded different IOPs ranging from 13 to 35 mmHg with an interval of 2 mmHg. To explore the effect of IOP on anterior and posterior corneal stress, the value of stress variation on the corneal surfaces under different IOPs was calculated. The results were showed in Figure 5.

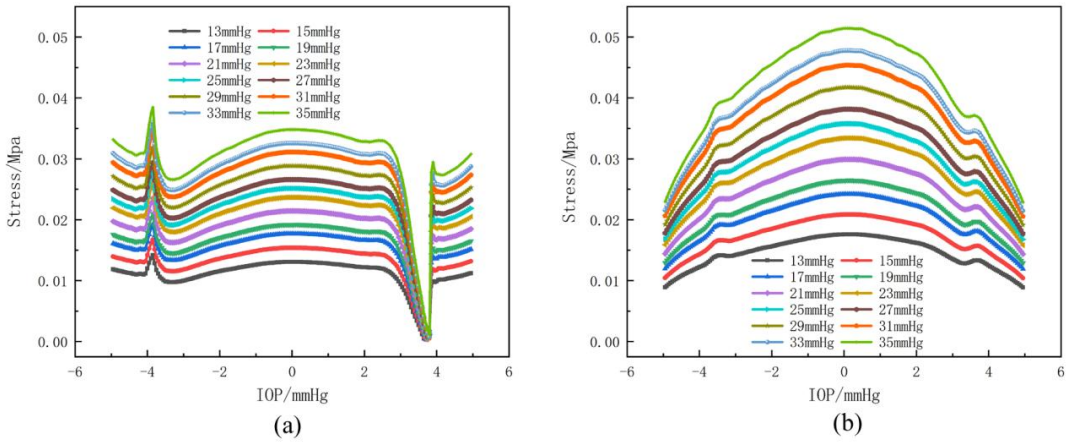

Figure 5. (a) The equivalent stress on the anterior surface of the cornea under different IOP. (b) The equivalent stress on the posterior surface of the cornea under different IOP. IOP ranged from 13 to 35 mmHg with intervals of 2 mmHg. The diopter was −6D.

In general, stress on the anterior and posterior surface of the cornea increased linearly with increasing IOP, whereas stress on the anterior surface of the cornea suddenly dropped to 0.001 MPa at the time of incision. According to Figure 5a, when the IOP was 13, 15 and 17 mmHg, the maximum stress were about 0.013, 0.015 and 0.017 MPa, respectively. Until the IOP was 35 mmHg, the maximum stress was 0.035 MPa. The result showed that the stress was increased by about 0.002 MPa at an interval of 2 mmHg. As observed in Figure 5b, the stress on the posterior surface of the cornea also increased linearly. When the IOP was 13, 15 and 17 mmHg, the maximum stress were about 0.017, 0.021 and 0.024 MPa, respectively. In conclusion, the stress on the posterior of the cornea increased by about 0.003 MPa with every 2 mmHg increase of IOP.

5.4. Effect of IOP on corneal surface equivalent strain

Different IOPs were applied to the eye model with a diopter of −6D and the equivalent strain on the corneal surface obtained. The IOP ranged from 13 to 35 mmHg with intervals of 2 mmHg. The results were as follows.

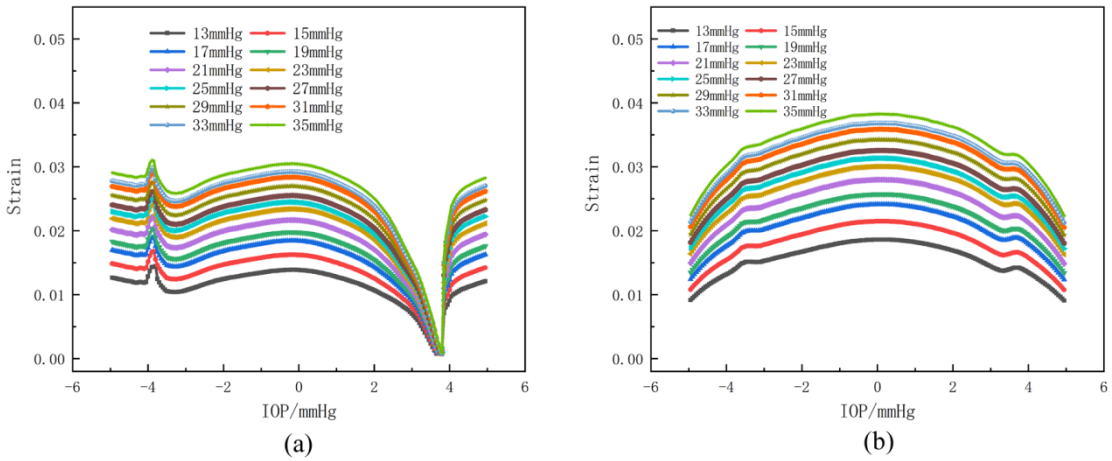

Figure 6. (a) The equivalent strain on the anterior surface of the cornea under different IOP. (b) The equivalent strain on the posterior surface of the cornea under different IOP. IOP ranged from 13 to 35 mmHg with intervals of 2 mmHg. The diopter was −6D.

Figure 6 indicated that the strain on the anterior and posterior surfaces of the cornea increased nonlinearly with increasing IOP. Different from the effect of IOP on corneal stress, the strain on the anterior surface of the cornea decreased slowly to 0.007 at the incision site. Figure 6a showed that the strain difference at the center decreased under the same IOP interval. When the IOP increased from 13 to 15 mmHg, the strain at the center increased by about 0.0025. The strain at the center increased by about 0.0022 from 15 to 17 mmHg. Between 17 and 19 mmHg, the strain at the center increased by about 0.0014. According to Figure 6b, when the IOP increased from 13 to 15 mmHg, the posterior cornea surface of strain at the center increased by about 0.0028. The strain at the center increased by about 0.0026 between 15 to 17 mmHg. In summary, the change of the strain on the posterior surface of the cornea was not linear with increasing IOP.

6. Discussion

6.1. Comparison with previous studies

The biomechanical response of the cornea is affected by eye diseases and surgical stability [25]. The flapless and small incision of SMILE refractive surgery has improved surgical safety [26]. Clinical studies have shown the biomechanical of corneal changed after surgery. Wu et al. [27] showed that corneal hysteresis and the corneal resistance factor both decreased, obviously changing the biomechanics of the corneal. Balidis et al. [28] showed that corneal biomechanics changed after SMILE. In addition, many studies showed that the stress and strain increased after surgery. Shih et al. [29] found that the central area of the cornea was the most deformed after SMILE. Franus et al. [8] also suggested that

the postoperative cornea was more deformed than the normal cornea. The finite element analysis has been used to research corneal biomechanics after refractive surgery. And the corneal biomechanics were also explored by modeling research. Shih et al. [29] used finite element method to simulate the changes of corneal shape and stress distribution after refractive surgical, which showed the changes of biomechanical cornea. Cordero showed that using a corneal model to analyze biomechanics were useful tools could quickly diagnose eye diseases [30]. NT Mohammad et al. [31] also used finite element model to assessing the mechanical behavior of the cornea. Therefore, previous studies have confirmed that corneal biomechanics changed after corneal refractive surgery. Our results suggested that postoperative corneal biomechanics might also change, the stress and strain increased. And the increases were concentrated in the central region after SMILE surgery. By constructing a 3D finite element model of the human eye and using computer algorithm to analyze the corneal biomechanics, our study had a certain theoretical significance for refractive surgery.

6.2. Effect of incision size on stress and equivalent strain

The sizes of incisions ranged from 2 to 5 mm with intervals of 0.5 mm. After applying 15 mmHg IOP, the stress and strain on the anterior surface of the cornea for different incision sizes were calculated. The results were showed in Figure 7.

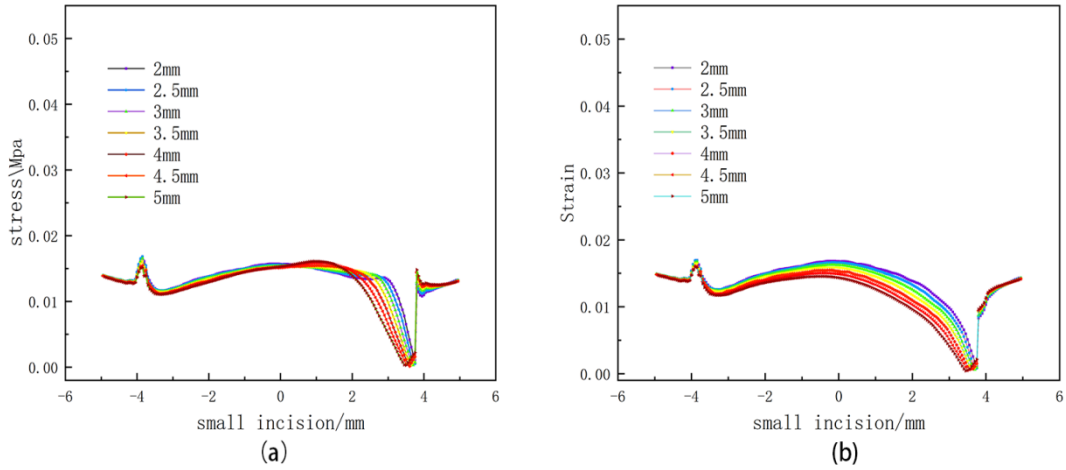

Figure 7. (a) Relationship between the sizes of incision and equivalent stress. (b) Relationship between the sizes of incision and equivalent strain. The incision size ranged from 2 to 5 mm, with an interval of 0.5 mm, and the diopter was −6D. IOP was 15 mmHg.

It was concluded from Figure 7 that the stress and strain on the anterior surface of the cornea increased with increasing incision size, and the changes were obviously at the incision site. Compared with diopter and IOP, incision size had little influence on corneal stress and strain. As observed in Figure 7a, the maximum stress in the central region was 0.016 MPa, and the change in value at the incision site was 0.001 MPa. According to Figure 7b, how strain and stress varies was consistent, and strain increased with increasing incision size. Overall, the incision size had only a slight effect on stress and strain in SMILE surgery, which might be associated with the small changes of corneal tension.

6.3. Equivalent stress on the X-axis at different diopters

Our results only considered stress in the Y-axis direction, but corneal stress in the X-axis direction should also be considered. Therefore, we calculated the X-axis direction stress changes on the anterior and posterior surfaces of the cornea under different diopters, ranging from 0D to −15D. The results were shown in Figure 8.

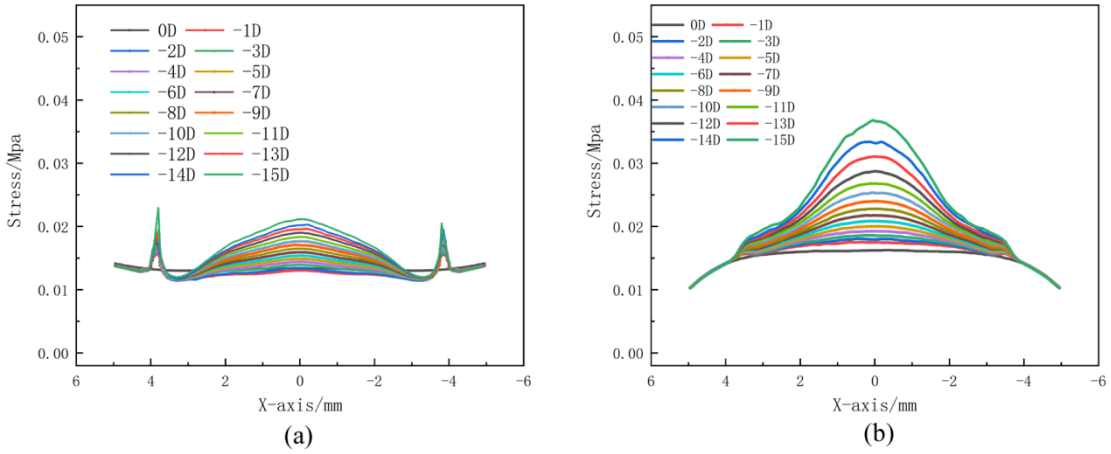

Figure 8. (a) The X-axis direction equivalent stress on the anterior surface of cornea under different corrected diopters. (b) The X-axis direction equivalent stress on the posterior surface of cornea under different corrected diopters. IOP was 15 mmHg.

Overall, stress also increased on the X-axis direction with increasing diopter. However, it was clear from Figure 8a that the stress on the anterior surface of the cornea was symmetrical, and no descent was observed at the incision location. The stress peaked at −3.8 and 3.8 mm due to the construction of the corneal cap and corneal dissociation. Figure 8b showed that the stress on the posterior surface of the cornea changed in a similar way to that on the Y-axis direction, and the stress on the posterior surface was greater than that on the anterior surface.

6.4. Other thoughts

Our study assessed the biomechanical responses of the cornea after SMILE surgery, which could provide references for the SMILE refractive surgery. But there were some imperfections that need to be improved. Firstly, SMILE surgery had a greater impact on the cornea, so our model was composed of the corneal cap, the cornea, and the sclera. However, in order to make the study results more accurate, the impact of other components should also be considered, which needed to be improved in future jobs. Secondly, the material properties of the cornea and sclera had also an important effect on the experimental results. Because of the nonlinear and hyperelastic properties of the cornea and sclera, the Ogden function model was selected. But there were individual differences in the human eye in clinical practice. Finally, we only considered the effects of the diopter, IOP, and incision size on stress and strain. In practice, the factors influencing stress and strain may included treatment decentration, material parameters, corneal ablation depth, and others. How all these factors influence corneal stress and strain required further exploration.

The biomechanics of ophthalmological procedures can be accurately analyzed by finite element analysis. Our next target is dynamic simulation of the clinical SMILE surgical procedure, so that our research findings will be closer to those of clinical surgery. Moreover, there are many factors that influence the outcome of surgery. We will study the postoperative biomechanics of the human eye from perspectives such as eye model, treatment decentration, and material parameters. Therefore, the finite element analysis used to study postoperative corneal biomechanics can provide a theoretical basis for making surgical plans and diagnosing postoperative ocular diseases after refractive surgery.

7. Conclusions

A 3D human eye model was used to simulate the SMILE surgery procedure based on the finite element analysis method, and we studied postoperative corneal stress and strain. Our results showed that with increasing corrected diopter, the equivalent stress and strain on the anterior and posterior surfaces of the cornea increased and were concentrated in the central area. However, compared with the anterior surface of the cornea, the changes in stress and strain on the posterior surface were significantly larger. With increasing IOP, corneal stress increased approximately linearly, whereas the strain increased nonlinearly. In addition, we found that the sizes and directions of incisions had a slight influence on stress and strain. In summary, our study indicated SMILE refractive surgery increased stress and strain, having certain influence on corneal biomechanics. And the result could guide the design of clinical operation and the avoidance of postoperation complications.

Acknowledgements

Supported by Natural National Science Foundation of China (NSFC) (61465010 & 81873684); National Key Research and Development Program of China (2018YFE0115700); Jiangxi Nature Science Foundation (20192BAB207035).

The authors thank the participants of this multicentre study for their valuable contributions.

The authors assume full responsibility for the analyses and interpretation of these data.

Conflict of interest

All authors declare no conflicts of interest in this paper.

References

1. J. Wang, X. Xun, D. O. Ophthalmology, S. G. Hospital, Environmental risk factors for myopia and advances in its control and prevention, *Shanghai Med. Pharm. J.*, **38** (2017), 3–7.
2. M. Kohlhaas, Corneal sensation after cataract and refractive surgery, *J. Cataract Refract. Surg.*, **24** (1998), 1399–1409.
3. D. Z. Reinstein, T. J. Archer, M. Gobbe, The Key characteristics of corneal refractive surgery: biomechanics, spherical aberration, and corneal sensitivity after SMILE, in *Small Incision Lenticule Extraction (SMILE)*, Springer, Cham, (2015), 123–142.
4. A. Gyldenkerne, A. Ivarsen, J. Hjortdal, Comparison of corneal shape changes and aberrations induced By FS-LASIK and SMILE for myopia, *J. Refractive Surg.*, **31** (2015), 223–229.

5. P. Wei, G. P. Cheng, J. Zhang, A.L. Ng, Y. Wang, Changes in corneal volume at different areas and its correlation with corneal biomechanics after SMILE and FS-LASIK surgery, *J. Ophthalmol.*, **2020** (2020), 1–7.
6. G. Scarcelli, S. H. Yun, Brillouin scanning microscopy in keratoconus, in *Keratoconus: Recent Advances in Diagnosis and Treatment*, Springer International Publishing, (2017), 167–173.
7. N. Cartwright, J. R. Tyrer, P. D. Jaycock, J. Marshall, Effects of variation in depth and side cut angulations in LASIK and thin-flap LASIK using a femtosecond laser: a biomechanical study, *J. Refractive Surg.*, **28** (2012), 419–425.
8. D. V. Franus, Change in the stress-strain state of the cornea after refractive surgery, in *2015 International Conference on Mechanics-Seventh Polyakhov's Reading*, IEEE, (2015), 1–4.
9. J. C. He, J. Gwiazda, F. Thorn, R. Held, Wave-front aberrations in the anterior corneal surface and the whole eye, *J. Opt. Soc. Am. A*, **20** (2003), 1155–1163.
10. A. S. Roy, W. J. Dupps, Effects of altered corneal stiffness on native and postoperative LASIK corneal biomechanical behavior: a whole-eye finite element analysis, *J. Refractive Surge.*, **25** (2009), 875–887.
11. K. J. Bathe, D. Chapelle, *Computational Fluid And Solid Mechanics: the Finite Element Analysis of Shells- Fundamentals*, Springer , 2003.
12. M. Á. Ariza-Gracia, J. F. Zurita, D. P. Pinero, J. F. Rodriguez, Coupled biomechanical response of the cornea assessed by non-contact tonometry, a simulation study, *PLOS ONE*, **10** (2015), e0121486.
13. M. Kaliske, A formulation of elasticity and viscoelasticity for fibre reinforced material at small and finite strains, *Comput. Methods Appl. Mech. Eng.*, **185** (2000), 225–243.
14. K. Anderson, A. El-Sheikh, T. Newson, Application of structural analysis to the mechanical behaviour of the cornea, *J. R. Soc. Interface*, **1** (2004), 1742–5662.
15. P. M. Pinsky, D. V. Datye, A microstructurally-based finite element model of the incised human cornea, *J. Biomech.*, **24** (1991), 907–922.
16. R. Shah, S. Shah, S. Sengupta, Results of small incision lenticule extraction: all-in-one femtosecond laser refractive surgery, *J. Cataract Refractive Surg.*, **37** (2011), 127–137.
17. J. B. Randleman, B. Russell, M. A. Ward, K. P. Thompson, R. D. Stulting, Risk factors and prognosis for corneal ectasia after LASIK, *Ophthalmology*, **110** (2003), 267–275.
18. K. A. John, Comparison of corneal biomechanics after myopic small-incision lenticule extraction compared to LASIK: an ex vivo study, *Clin. Ophthalmol.*, **12** (2018), 237–245.
19. I. M. Osman, H. A. Helaly, M. Abdalla, M. A. Shousha, Corneal biomechanical changes in eyes with small incision lenticule extraction and laser assisted in situ keratomileusis, *BMC Ophthalmol.*, **16** (2016), 123.
20. T. F. Peinado, D. P. Piñero, I. A. López, J. L. Alio, Correlation of both corneal surfaces in corneal ectasia after myopic LASIK, *Optom. Vision Sci.*, **88** (2011), E539–E542.
21. R. Grytz, K. Krishnan, R. Whitley, V. Libertiaux, J. C. Downs, A mesh-free approach to incorporate complex anisotropic and heterogeneous material properties into eye-specific finite element models, *Comput. Methods Applied Mech. Eng.*, **358** (2020), 112654.
22. J. G. Yu, F. J. Bao, Y. F. Feng, C. Whitford, A. Elsheikh, Assessment of corneal biomechanical behavior under posterior and anterior pressure, *J. Refractive Surg.*, **29** (2013), 64–70.
23. L. Fang, The influence of the aspheric profiles for transition zone on optical performance of human eye after conventional ablation, *J. Eur. Opt. Soc. Rapid Publ.*, **9** (1990).

24. C. J. Roberts, W. J. Dupps, Biomechanics of corneal ectasia and biomechanical treatments, *J. Cataract Refractive Surg.*, **40** (2014), 991–998.
25. M. Girard, W. J. Dupps, M. Baskaran, G. Scarcelli, S. H. Yun, H. A. Quigley, et al., Translating ocular biomechanics into clinical practice: current state and future prospects, *Curr. Eye Res.*, **40** (2015), 1–18.
26. S. Ganesh, S. Brar, R. R. Arra, Refractive lenticule extraction small incision lenticule extraction: a new refractive surgery paradigm, *Indian J. Ophthalmol.*, **66** (2018), 10–19.
27. W. Di, Y. Wang, L. Zhang, S. Wei, T. Xin, Corneal biomechanical effects: Small-incision lenticule extraction versus femtosecond laser ‐ assisted laser in situ keratomileusis, *J. Cataract Refractive Surg.*, **40** (2014), 954–962.
28. M. Balidis, Biomechanical profile of refractive surgery procedures, *Acta Ophthalmol.*, **97** (2019).
29. P. J. Shih, I. J. Wang, W. F. Cai, J. Y. Yen, Biomechanical simulation of stress concentration and intraocular pressure in corneas subjected to myopic refractive surgical procedures, *Sci. Rep.*, **7** (2017), 13906.
30. M. I. Cordero-Mendieta, E. Pinos-V ́ez, R. Coronel-Berrezueta, Study of corneal biomechanics and modeling of Young's module in healthy and pathological corneas, in *International Conference on Applied Human Factors and Ergonomics*, Springer, Cham, (2020), 99–105.
31. N. T. Mohammad, F. Craig, G. Dipika, Finite element modelling of cornea mechanics: a review, *Arq. Bras. Oftalmol.*, **77** (2014), 60–65.

AIMS Press